THIS MONTH IN
JNM

Prostate cancer imaging: Zaheer and colleagues provide an overview of key clinical issues in prostate cancer imaging and therapy and summarize molecular modalities and agents with promise for future applications. . . . . ***Page 1387***

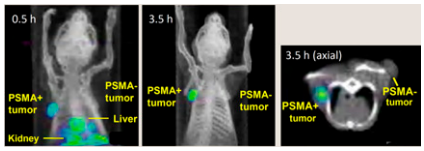

Molecular imaging of cartilage: Sarda-Mantel and Le Guludec review current cartilage imaging approaches in arthrosis and chondrosarcoma, with a focus on the potential for cartilage proteoglycan targeting. . . . . ***Page 1391***

PSA and PET/CT detection rate: Castellucci and colleagues investigate the effect of various prostate-specific antigen parameters on the ^{11}C-choline PET/CT detection rate in patients with biochemical failure after radical prostatectomy for prostate cancer. . . . . ***Page 1394***

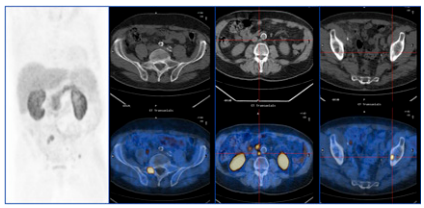

Dedicated breast PET/CT: Bowen and colleagues perform initial performance characterization studies of a dedicated breast PET/CT device capable of high-resolution functional and anatomic imaging. . . . .***Page 1401***

Optimizing injected activity in PET: Walker and colleagues report on a generalized method for maximizing the statistical quality of dynamic PET images by optimizing injected activity in a patient-, tracer-, and body region–specific manner. . . ***Page 1409***

Cardiac segmentation QC for SPECT: Xu and colleagues describe a technique to automatically detect failures in accurate assessment of left ventricular contours for both gated and nongated myocardial perfusion SPECT studies. . . . . ***Page 1418***

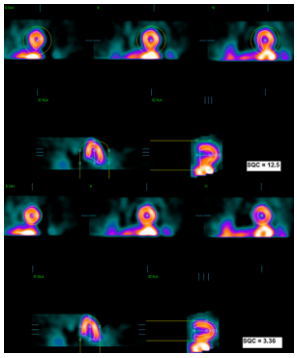

PET for monitoring PRRT: Gabriel and colleagues compare ^{68}Ga-DOTA-TOC PET with CT or MRI for assessing treatment response to peptide-related radionuclide therapy in patients with advanced neuroendocrine tumors. . . . . ***Page 1427***

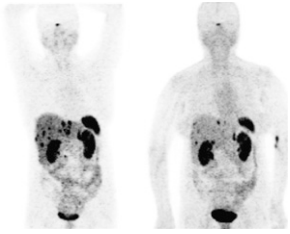

PET and osteosarcoma response: Cheon and colleagues evaluate the usefulness of ^{18}F-FDG PET in predicting histologic responses to neoadjuvant chemotherapy before surgical resection and thereby enhancing individualized treatment planning and management. . . . . ***Page 1435***

^{18}F-FLT PET in HCC imaging: Eckel and colleagues investigate the ability of PET to detect hepatocellular carcinoma in patients with clinically suspected disease and discuss the potential utility of resulting uptake data to provide useful prognostic information. . . . . ***Page 1441***

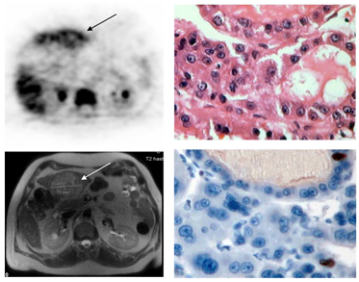

^{123}I-MIBG imaging of pheochromocytoma: Wiseman and colleagues report on a study designed to validate the performance of ^{123}I-MIBG scintigraphy in the evaluation of patients with known or suspected primary or metastatic pheochromocytoma or paraganglioma. . . . . ***Page 1448***

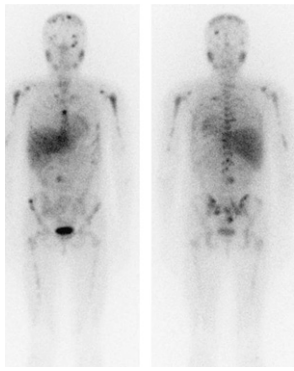

Imaging nicotinic receptors in dementia: Mitsis and colleagues use ^{123}I-5-IA-85380 SPECT to compare nicotinic receptor availability in various brain regions in individuals with Alzheimer disease or mild cognitive impairment and in healthy controls. . . . . ***Page 1455***

CSF and PET tracer binding: Tolboom and colleagues explore potential relationships between cerebrospinal fluid measurements of β-amyloid-1–42 and total tau to ^{11}C-PiB and ^{18}F-FDDNP binding as measured with PET and discuss the implications of their findings. . . . . ***Page 1464***

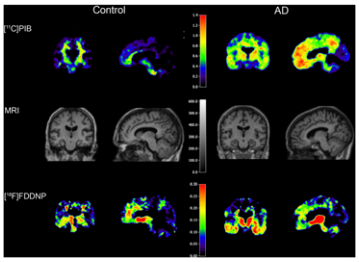

Misregistration and attenuation-corrected MPI: Kennedy and colleagues detail the incidence, direction, magnitude, and effects of misregistration between SPECT and CT in CT-based attenuation-corrected myocardial perfusion imaging studies. . . . . ***Page 1471***

Hypertension and fluorodopa uptake: Goldstein and colleagues describe a study designed to determine whether supine hypertension increases 6-^{18}F-fluorodopa uptake on PET, potentially confounding identification of striatal dopaminergic denervation in Parkinson disease and other settings. . . . ***Page 1479***

Pediatric PET/CT dosimetry: Fahey provides an educational overview of the physical aspects of PET, CT, and hybrid imaging in children and provides practical insights on approaches to keeping radiation doses as low as practical without compromising the quality of care. . . ***Page 1483***

Small protein for *HER2* imaging: Ren and colleagues describe the development of and initial studies with an Affibody-derived small 2-helix protein scaffold as a promising PET probe for in vivo imaging of human epidermal growth factor receptor type 2 expression. . . . . ***Page 1492***

PET targeting of CD20: Olafsen and colleagues detail the development of anti-CD20 antibody fragments for immunoPET imaging in preclinical studies of non-Hodgkin lymphoma. . . . . ***Page 1500***

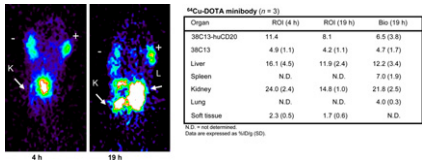

Novel radioligands for serotonin transporters: Wang and colleagues outline the development and refinement of a series of ^{18}F-labeled agents for PET imaging of serotonin transporters and elucidation of both normal physiologic and disease states. . . . ***Page 1509***

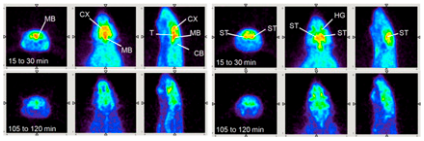

Dosimetry for ^{131}I-MIBG therapy: Buckley and colleagues examine the relationship between whole-body absorbed dose and hematologic toxicity and assess the most accurate method for delivering a prescribed whole-body absorbed dose in ^{131}I-MIBG treatment for neuroblastoma. . . . ***Page 1518***

PET and prognosis in HCC: Ahn and colleagues describe in vitro studies exploring the ways in which aspects of ^{18}F-FDG uptake on PET, especially relating to overexpression of hexokinase II, are linked to tumor proliferation mechanisms in hepatocellular carcinoma. . . . ***Page 1525***

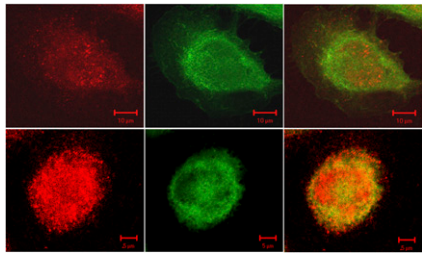

SUV and chemotherapy response: Dutour and colleagues investigate whether ^{18}F-FDG PET could be a noninvasive surrogate for histopathologic analysis in osteosarcoma, facilitating earlier response evaluation to neoadjuvant chemotherapy. . . . ***Page 1533***

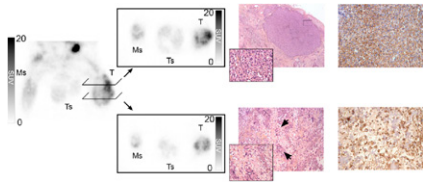

Imaging cartilage tumor tissue: Miot-Noirault and colleagues report on an animal study designed to determine whether a novel ^{99m}Tc-labeled tracer that binds to cartilage proteoglycans has potential for scintigraphic imaging of cartilage tumoral tissue. . . . . ***Page 1541***

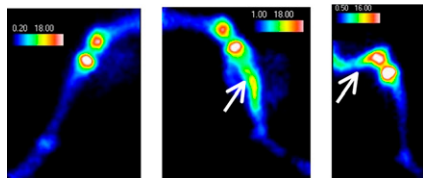

Converging collimators in brain SPECT: Ter-Antonyan and colleagues describe a project undertaken to increase the sensitivity of a triple-camera SPECT system and reduce statistical noise in reconstructed human brain images using a combination of converging collimators. . . . . ***Page 1548***

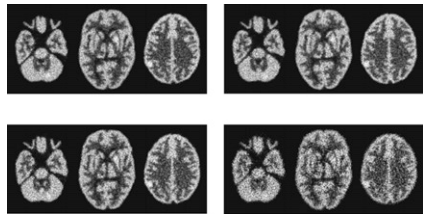

ON THE COVER

Scanning of the uncompressed breast with dedicated breast PET/CT can accurately show suspected lesions in 3 dimensions. Pictured here are the CT, PET, and fused images of a 49-y-old patient who presented with a palpable, mammographically evident 23-mm irregular focal mass at the 8 o'clock position. In the fused axial image, 3 separate foci of uptake as seen on PET are shown overlying fibroglandular tissue as seen on CT.

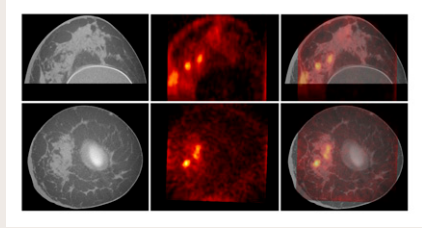

See page 1406.